J Eng Math (2014) 85:83–97
DOI 10.1007/s10665-013-9626-9

Eigenoscillations of a thin-walled azimuthally closed, axially open shell of revolution

I. Gavrilyuk · M. Hermann · V. Trotsenko · Yu. Trotsenko · A. Timokha

Received: 5 May 2012 / Accepted: 21 January 2013 / Published online: 15 May 2013

Abstract This paper generalizes earlier authors' results on the analytical approximation of the singularly perturbed boundary problem describing the eigenoscillations of a thin-walled axisymmetric shell. The asymptotic behavior of the eigenmodes at the clamped ends is studied, and a set of trial functions capturing this behavior is constructed to be used in the Ritz method. Illustrative numerical examples demonstrate a fast convergence so that the eigenmodes are accurately approximated in a uniform metric together with their second-, third-, and fourth-order derivatives. The numerical results are validated by comparing them with an asymptotic eigensolution and computations done by the ANSYS codes based on the finite-element method.

Keywords Singularly perturbed problems · Thin-walled shell · Variational methods

The literature contains a variety of analytical and numerical approaches to the problem of forced and eigenoscillations of thin-walled shells. In our previous paper [1], where a semianalytical approach was developed to solve the problem of axisymmetric eigenoscillations of a closed shell of revolution, a short survey referred readers to [2–6]. The present paper focuses on thin-walled azimuthally closed, axially open axisymmetric shells. Because there is a broader set of publications for this shell shape associated, first of all, with cylindrical and conical shells, one should extend the reference list to include the fundamental works [7–15].

Our research goal consists of generalizing the semianalytical approach [1] to the spectral boundary problem on eigenoscillations of a thin-walled azimuthally closed, but axially open, axisymmetric shell. This implies establishing analytical features of the eigenmodes, which includes a description of the boundary layer behavior at the shell ends,

I. Gavrilyuk
Berufsakademie Eisenach-Staatliche Studienakademie Thüringen, University of Cooperative Education, Am Wartenberg 2, 99817 Eisenach, Germany

M. Hermann
Friedrich-Schiller-Universität Jena, Ernst-Abbe-Platz 1-2, 07745 Jena, Germany

V. Trotsenko · Yu. Trotsenko · A. Timokha
Institute of Mathematics, National Academy of Sciences of Ukraine, 3 Tereschenkivska Street, Kiev 01601, Ukraine

A. Timokha (✉)
Centre for Autonomous Marine Operations and Systems (AMOS), Department of Marine Technology, Norwegian University of Science and Technology, 7491Trondheim, Norway
e-mail: alexander.timokha@ntnu.no

and developing the Ritz scheme, which constructs an approximate eigensolution possessing the aforementioned boundary layer behavior. The Ritz approximation should provide convergence to the eigenmodes, together with the first- to fourth-order derivatives. This will facilitate computation of the bending force and moment.

The studied spectral boundary problem involves a system of ordinary differential equations (ODEs) within a small parameter in the front of the highest-order derivative. This means that we deal with the so-called *singularly perturbed* problem, whose solutions are difficult to approximate by employing traditional numerical tools. It is the same as in [1]. A novelty is that, because antisymmetric eigenmodes are of concern for thin-walled azimuthally closed, axially open axisymmetric shells, separation of the angular variable yields the governing ODEs, which are parametrically dependent on the "angular" integer number n. This means that the analytical properties of the eigenmodes are different from those in [1]. Furthermore, there exist the two shell end conditions for the axially open axisymmetric shells.

For the studied shell shape, an asymptotic eigensolution in terms of the nondimensional shell thickness was constructed, e.g., in [16,17] based on Koiter's shell equations. Bearing in mind our previous paper [1], we adopt the technical theory of shells. However, the proposed semianalytical approach can be extended to other shell equations as well as different boundary conditions. To get an accurate approximation of the eigenmodes for the realistic thickness, the approach constructs the boundary layer trial functions and employs them in the Ritz scheme together with the Legendre polynomials. A bonus is that this approximation guarantees the uniform convergence to the second-, third-, and forth-order derivatives that are involved in computing the bending forces and moments.

Section 1 starts by formulating the spectral boundary problem on the eigenoscillations of shells, which is well known from other publications. The technical theory of shells is adopted with clamped boundary conditions. This is to be consistent with earlier studies in [1] and, of course, for brevity's sake.

The eigenmodes and their analytical features are studied in Sect. 2. Based on these studies, a set of trial functions that possess the boundary layer behavior at shell edges is constructed. This set is parametrically dependent on the unknown eigenfrequencies, and therefore, employing them in numerical methods requires a special iterative procedure. Section 3 develops the corresponding iterative Ritz scheme employing the constructed trial functions. Numerical experiments for cylindrical and conical shells are reported in Sect. 4. The results are validated by comparison with Nau and Simmonds [17] and finite-element calculations by means of ANSYS codes. Whereas the Ritz method uses exclusively a regular basis (represented by the Legendre polynomials), it gives a quite fast stabilization of significant figures for the eigenvalues, but the approximate eigenmodes are found with a reasonable error in the vicinity of the shell ends. Including the constructed trial functions provides an accurate uniform approximation of the eigenmodes and their higher-order derivatives for a broad range of the shell thickness values. Even though [17] employs the Koiter equations of shells, the asymptotic solution calculations in [17] are consistent with our approximate results based on the technical theory of shells. A discrepancy becomes nonnegligible only with increasing shell thickness. Our calculations on eigenfrequencies are also consistent with those following from the ANSYS codes when the latter are conducted with a relatively small shell thickness.

1 Problem statement

We consider linear-free oscillations of a thin-walled azimuthally closed, axially closed axisymmetric shell as shown in Fig. 1. Along with the $Or\theta Z$ cylindrical coordinate system, we consider the lines of longitude (meridians) parameterized by the natural meridian-length parameter s ($s_1 \leqslant s \leqslant s_2$) and the corresponding natural local coordinate system in which longitudinal, latitudinal, and normal small-magnitude displacements of the midsurface are defined by U, V, and W, respectively. Figure 1 demonstrates these displacements as well as the coordinate r of the shell midsurface, which is, in fact, the distance $r = r(s)$ between a midsurface point and the symmetry axis. Pursuing a compact formulation of the corresponding boundary value problem on the linear-free shell oscillation, we introduce two variables, $R_1 = R_1(s)$ and $R_2 = R_2(s)$, which define the two principal curvatures of the shell. The first principal curvature $R_1(s)$ is associated with curvatures of the meridional curves; the second principal curvature $R_2(s)$ equals the distance between the midsurface and the symmetry axis measured along the normal line.

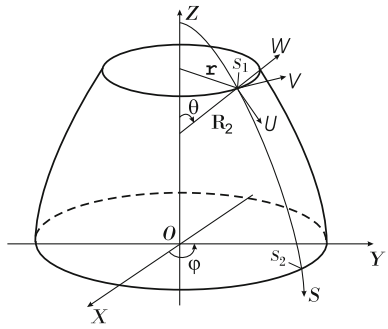

Fig. 1 Sketch of thin-walled azimuthally closed, axially closed axisymmetric shell. Along with the $Or\theta Z$ cylindrical coordinate system, we introduce the local coordinate system at the midsurface shell points in which U, V, and W imply, respectively, longitudinal, latitudinal, and normal displacement of the freely oscillating shell. The s-longitudinal variable gives the natural parameterization of the *lines* of longitude; it changes from s_1 to s_2. The variable R_2 is the distance between the midsurface and the symmetry axis measured along the normal *line*, and θ is the angle between the normal *line* and the OZ-axis

Eigenoscillations of the axisymmetric shell are studied implying separation of the spatial coordinates and time as follows:

$$U(s,\varphi,t)=\mathrm{e}^{\mathrm{i}\omega t}u(s)\cos n\varphi,\ \ V(s,\varphi,t)=\mathrm{e}^{\mathrm{i}\omega t}v(s)\sin n\varphi,\ \ W(s,\varphi,t)=\mathrm{e}^{\mathrm{i}\omega t}w(s)\cos n\varphi. \tag{1}$$

Here $\mathrm{i}=\sqrt{-1}$, $\mathbf{u}(s)\equiv(u(s),v(s),w(s))^T$ is the *eigenmode*, and ω is the *eigenfrequency*. After choosing a characteristic shell radius R_0, which can be either upper or lower or mean radius of the shell, and introducing the shell thickness h, the Young modulus E, the Poisson coefficient ν, and the shell density ρ, we define the characteristic time $\sqrt{(1-\nu^2)\rho^2R_0/E}$ and focus on a nondimensional formulation of the problem. The nondimensional *eigensolution* ($\mathbf{u}$ and ω) satisfies the following ODEs (Chaps. 5 [2] and 10 [18]):

$$A\mathbf{u}-\lambda\mathbf{u}=\mathbf{0},\quad A\equiv c^2K+L,\quad c^2\equiv\frac{h^2}{12R_0^2},\quad \lambda\equiv\frac{(1-\nu^2)\rho R_0^2\omega^2}{E}. \tag{2}$$

Here the components of the matrix operator $L=\{L_{ij}\}$ are as follows:

$$L_{11}=-\frac{\mathrm{d}}{\mathrm{d}s}\frac{1}{r}\frac{\mathrm{d}}{\mathrm{d}s}r+\frac{1-\nu}{2}\left(\frac{n^2}{r^2}-\frac{2}{R_1R_2}\right),\qquad L_{12}=-n\frac{\mathrm{d}}{\mathrm{d}s}\frac{1}{r}+\frac{1-\nu}{2}\frac{n}{r^2}\frac{\mathrm{d}}{\mathrm{d}s}r,$$

$$L_{13}=\frac{1-\nu}{R_2}\frac{\mathrm{d}}{\mathrm{d}s}-\frac{\mathrm{d}}{\mathrm{d}s}\left(\frac{1}{R_1}+\frac{1}{R_2}\right),\qquad L_{22}=\left(\frac{n^2}{r^2}-\frac{1-\nu}{R_1R_2}\right)-\frac{(1-\nu)}{2}\frac{\mathrm{d}}{\mathrm{d}s}\frac{1}{r}\frac{\mathrm{d}}{\mathrm{d}s}r,$$

$$L_{23}=\frac{n}{r}\left(\frac{\nu}{R_1}+\frac{1}{R_2}\right),\qquad L_{31}=\frac{1}{r}\left(\frac{1}{R_1}+\frac{1}{R_2}\right)\frac{\mathrm{d}}{\mathrm{d}s}r-\frac{1-\nu}{r}\frac{\mathrm{d}}{\mathrm{d}s}\frac{r}{R_2},$$

$$L_{32}=\frac{n}{r}\left(\frac{\nu}{R_1}+\frac{1}{R_2}\right),\qquad L_{33}=\frac{1}{R_1^2}+\frac{2\nu}{R_1R_2}+\frac{1}{R_2^2},$$

$$L_{21}=\frac{n}{r^2}\frac{\mathrm{d}}{\mathrm{d}s}r-\frac{(1-\nu)n}{2}\frac{\mathrm{d}}{\mathrm{d}s}\frac{1}{r},$$

where $r(s)$, $R_1(s)$, and $R_2(s)$ are known functions of s, $s_1\le s\le s_2$. Furthermore, the matrix operator $K=\{K_{ij}\}$ contains the nondimensional parameter c^2, which vanishes as h/R_0 tends to zero. The operator deals with the second-order derivatives for $i,\ j\leqslant 2$, the third-order derivatives for $2<i+j<6$, and the fourth-order derivatives for $i=j=3$, respectively.

Bearing in mind the authors' earlier results on closed shells of revolution [1] and pursuing a succession between [1] and the present paper, we will furthermore adopt the *technical theory* of shells and the Kirchhoff–Love kinematic model (Chap. 10 [18] and [1]) implying

$$K_{ij}=0\quad\text{for } i+j<6,\ \ K_{33}=\Delta_n\Delta_n+\frac{1-\nu}{r}\left(\frac{\mathrm{d}}{\mathrm{d}s}\frac{r}{R_1R_2}\frac{\mathrm{d}}{\mathrm{d}s}-\frac{n^2}{rR_1R_2}\right),\quad \Delta_n=\frac{1}{r}\frac{\mathrm{d}}{\mathrm{d}s}r\frac{\mathrm{d}}{\mathrm{d}s}-\frac{n^2}{r^2}. \tag{3}$$

One should note that the technical theory of shells can be poor for predicting beam-type eigenmodes corresponding to $n = 1$. More accurate theories of cylindrical shells are exemplified by Koiter's equations [11,12], which replace Δ_n in (3) by $\mathrm{d}^2/\mathrm{d}s^2 - n^2 + 1$. The latter expression was adopted in [17] for constructing an asymptotic solution of the corresponding spectral boundary problem based on (2). However, we will show in Sect. 4 that results by Nau and Simmonds [17] are consistent with our results based on the technical theory of shells.

Furthermore, we concentrate on the clamped shell ends suggesting the boundary conditions

$$u = v = w = \frac{\mathrm{d}w}{\mathrm{d}s} = 0 \quad \text{for} \quad s = s_1, s_2 \tag{4}$$

on both sides of an axisymmetric shell. Even though these conditions can appear in many practical problems (the authors have encountered them in modeling multicomponent beam-shell mechanical systems [19]), they look, to some extent, artificial, used for simplifying the analytical derivations below. The reported analytical studies can, however, be extended to other boundary conditions, if required.

2 Asymptotic behavior of eigenmodes

The ODEs (2) reduce to the following differential equation with respect to $w(s)$:

$$\mu^{m-l} N(w) - M(w) = 0, \qquad N(w) \equiv \sum_{k=0}^{m} a_{m-k}(s) \frac{\mathrm{d}^k w}{\mathrm{d}s^k}, \qquad M(w) \equiv \sum_{k=0}^{l} b_{l-k}(s) \frac{\mathrm{d}^k w}{\mathrm{d}s^k}, \quad m > l, \tag{5}$$

where $m = 8$ and $l = 4$ for antisymmetric eigenmodes ($n \neq 0$) and $m = 6$ and $l = 2$ for axisymmetric eigenmodes ($n = 0$). For cylindrical, conical, and other shell shapes, $a_i(s)$ and $b_i(s)$ are known analytical functions of s on $s_1 \leqslant s \leqslant s_2$, and

$$a_0(s) \equiv 1, \quad b_0(s) = \lambda - (1 - \nu^2)/R_2^2. \tag{6}$$

Equation (5) contains the small parameter $c^2 = \mu^{m-l}$ at the highest-order derivative. To get an analytical asymptotic solution, we assume that

$$b_0(s) < 0 \quad \text{for } s_1 \leqslant s \leqslant s_2, \tag{7}$$

which implicitly means that λ corresponds to a lower eigenvalue.

Employing the general theory of singularly perturbed problems [20–22], we postulate linearly independent solutions of (5) in the form

$$w_j(s, \mu) = \sum_{p=0}^{\infty} \mu^{p(m-l)} w_{j,p}(s). \tag{8}$$

Substituting (8) into (5) and comparing coefficients at the lowest power of μ leads to the linear ODE $M(w_{j,0}(s)) = 0$, where $w_{j,0}(s)$, $j = 1, 2, \ldots, l$, where l is the number of linearly independent solutions. Obviously, the higher-order approximations $w_{j,p}(s)$ can be found by gathering the terms at the higher-order powers of μ, which leads to the recursion formula

$$M(w_{j,p}(s)) = N(w_{j,p-1}(s)), \quad p = 1, 2, \ldots. \tag{9}$$

Here, the right-hand side depends on the already determined functions $w_{j,p-1}(s)$ starting with $w_{j,0}(s)$, $j = 1, \ldots, l$.

Hence, representation (8) gives l *linearly independent analytical solutions* on the interval $s_1 \leqslant s \leqslant s_2$, $j = 1, 2, \ldots, l$. Explicit analytical expressions for the lower-order terms of (8) (for particular shell shapes) can be found, e.g., in [23–26].

To find all the remaining $(m - l)$ linearly independent solutions, we use the representation

$$w_{l+j}(s, \mu) = \sum_{p=0}^{\infty} \mu^p w_{l+j,p}(s) \exp\left\{ \frac{1}{\mu} \int_{s_0}^{s} \varphi_j(t) \mathrm{d}t \right\}, \quad j = 1, 2, \ldots, (m - l), \quad s_0 \in [s_1, s_2]. \tag{10}$$

Substituting (10) into (5) and equating the terms at the same powers of μ leads to the functions $w_{l+j,p}(s)$ and $\varphi_j(t)$. In particular, if we take the terms with μ^{-l}, the following equation appears with respect to $\varphi_j(s)$:

$$(\varphi_j(s))^{m-l} - b_0(s) = 0, \tag{11}$$

which has four different roots:

$$\varphi_1(s) = \frac{-1+\mathrm{i}}{\sqrt{2}}|b_0|^{1/4}, \quad \varphi_2(s) = \frac{-1-\mathrm{i}}{\sqrt{2}}|b_0|^{1/4}, \quad \varphi_3(s) = \frac{1+\mathrm{i}}{\sqrt{2}}|b_0|^{1/4}, \quad \varphi_4(s) = \frac{1-\mathrm{i}}{\sqrt{2}}|b_0|^{1/4}. \tag{12}$$

Furthermore, the terms at μ^{-l+1} yield a linear homogeneous ODE with respect to $w_{l+j,0}(s)$, and the terms at μ^{-l+1+p}, $p = 1, 2, \ldots$, give linear ODEs with respect to $w_{l+j,p}(s)$ whose left-hand side is the same as for $w_{l+j,0}(s)$, but the right-hand side contains expressions that depend on $w_{l+j,k}(s)$ $(k < p)$ and their derivatives. One can show that the functions $w_{l+j,p}(s)$ in (10) are analytical on the considered interval and can therefore be expressed as a Taylor series in neighborhoods of $s = s_1$ and $s = s_2$, respectively.

Substituting (12) into the multiplier $\exp\frac{1}{\mu}\int_{s_0}^{s}\varphi_j(t)\mathrm{d}t$ (with $s = s_1$ and $s = s_2$) and separating the real and imaginary parts gives the following two linearly independent solutions:

$$\mathrm{e}^{\beta_k(s)}\cos\beta_k(s) \quad \text{and} \quad \mathrm{e}^{\beta_k(s)}\sin\beta_k(s), \quad k = 1, 2, \quad \text{where} \quad \beta_k(s) \equiv \frac{(-1)^k}{\mu\sqrt{2}}\int_{s_k}^{s}|b_0(t)|^{1/4}\mathrm{d}t. \tag{13}$$

They imply boundary layer behavior since, for $k = 1$ and $(s - s_1) \geq O(\mu)$, the functions $\mathrm{e}^{\beta_1(s)}\cos\beta_1(s)$ and $\mathrm{e}^{\beta_1(s)}\sin\beta_1(s)$ decay rapidly, but for $k = 2$ and $(s_2 - s) \geq O(\mu)$ they have only a small influence on the entire solution behavior. The boundary layers at s_k are therefore of the order $O(\mu)$.

In summary, taking together the linearly independent solutions (8) and (10) leads to the conclusion that the expression

$$\begin{aligned} f(s) = {} & \sum_{i=0}^{\infty} f_{i,0}s^i + \mathrm{e}^{\beta_1(s)}\cos\beta_1(s)\sum_{i=0}^{\infty} f_{i,1}(s-s_1)^i + \mathrm{e}^{\beta_1(s)}\sin\beta_1(s)\sum_{i=0}^{\infty} f_{i,2}(s-s_1)^i \\ & + \mathrm{e}^{\beta_2(s)}\cos\beta_2(s)\sum_{i=0}^{\infty} f_{i,3}(s-s_2)^i + \mathrm{e}^{\beta_2(s)}\sin\beta_2(s)\sum_{i=0}^{\infty} f_{i,4}(s-s_2)^i \end{aligned} \tag{14}$$

stands for $u(s)$, $v(s)$, and $w(s)$, where $f_{i,j}$ are unknown coefficients depending on μ. Solution (14) should satisfy the clamped-end boundary conditions, which yield additional restrictions for $f_{i,j}$.

Even though b_0 is, normally, an analytically given function determined by the shell shape, the functions $\beta_k(s)$ cannot generally be expressed in terms of elementary or special functions. In that case, as remarked in [27], one can admit the alternative analytical representations

$$\begin{aligned} w_{l+j}(s,\mu) &= \sum_{p=0}^{\infty}\mu^p P_j^{(p)}(\tau)\exp\{\varphi_j(s_1)\tau\}, \quad \tau = \frac{s-s_1}{\mu}, \quad \mathrm{Re}\varphi_j < 0, \\ w_{l+j}(s,\mu) &= \sum_{p=0}^{\infty}\mu^p P_j^{(p)}(\tau)\exp\{\varphi_j(s_2)\tau\}, \quad \tau = \frac{s_2-s}{\mu}, \quad \mathrm{Re}\varphi_j > 0, \end{aligned} \tag{15}$$

where $P_j^{(p)}(\tau)$ are the Vishik–Lusternik polynomials in τ of the order $2p$ whose coefficients are functions of $a_i(s)$ and $b_i(s)$ and their derivatives at $s = s_1$ and $s = s_2$. When Eqs. (15) are used, the functions β_k in (14) must be replaced by $(-1)^k|b_0(s_k)|^{1/4}(s_k - s)/(\sqrt{2}\mu)$.

3 Using the Ritz method to obtain a semianalytical solution

Functions u, v, and w restricted to (4) satisfy the variational equation [1]

$$\delta I = \int_{s_1}^{s_2} \Big[\Psi_{11}(u,\delta u) + \Psi_{12}(v,\delta u) + \Psi_{13}(w,\delta u) + \Psi_{12}(\delta v, v) + \Psi_{22}(v,\delta v) + \Psi_{23}(w,\delta v) + \Psi_{13}(\delta w, u) + \Psi_{23}(\delta w, v) + \Psi_{33}(w,\delta w) \Big] r\,\mathrm{d}s - \lambda \int_{s_1}^{s_2} (u\delta u + v\delta v + w\delta w) r\,\mathrm{d}s = 0, \tag{16}$$

with trial functions δu, δv, and δw subject to (4), where

$$\Psi_{11}(p,q) = \left(\frac{\cos^2\theta}{r^2} + \frac{\nu_1 n^2}{r^2}\right) pq + \left(\frac{\mathrm{d}p}{\mathrm{d}s} + \frac{\nu\cos\theta}{r}p\right)\frac{\mathrm{d}q}{\mathrm{d}s} + \frac{\nu\cos\theta}{r}\frac{\mathrm{d}p}{\mathrm{d}s}q,$$

$$\Psi_{12}(p,q) = \left(\frac{n\cos\theta}{r^2} + \frac{\nu_1 n\cos\theta}{r^2}\right) pq + \frac{\nu n}{r}p\frac{\mathrm{d}q}{\mathrm{d}s} - \frac{\nu_1 n}{r}q\frac{\mathrm{d}p}{\mathrm{d}s},$$

$$\Psi_{23}(p,q) = \left(\frac{n\sin\theta}{r^2} + \frac{\nu n}{rR_1}\right) pq,$$

$$\Psi_{13}(p,q) = \left(\frac{1}{R_1} + \frac{\nu\sin\theta}{r}\right) p\frac{\mathrm{d}q}{\mathrm{d}s} + \left(\frac{\cos\theta\sin\theta}{r^2} + \frac{\nu\cos\theta}{rR_1}\right) pq,$$

$$\Psi_{22}(p,q) = \left(\frac{n^2}{r^2} + \frac{\nu_1\cos^2\theta}{r^2}\right) pq + \left(\nu_1\frac{\mathrm{d}p}{\mathrm{d}s} - \frac{\nu_1\cos\theta}{r}p\right)\frac{\mathrm{d}q}{\mathrm{d}s} - \frac{\nu_1\cos\theta}{r}\frac{\mathrm{d}p}{\mathrm{d}s}q,$$

$$\Psi_{33}(p,q) = c^2\Bigg[\frac{\mathrm{d}^2p}{\mathrm{d}s^2}\frac{\mathrm{d}^2q}{\mathrm{d}s^2} + \frac{\nu\cos\theta}{r}\left(\frac{\mathrm{d}^2p}{\mathrm{d}s^2}\frac{\mathrm{d}q}{\mathrm{d}s} + \frac{\mathrm{d}^2q}{\mathrm{d}s^2}\frac{\mathrm{d}p}{\mathrm{d}s}\right) - \frac{\nu n^2}{r^2}\left(\frac{\mathrm{d}^2p}{\mathrm{d}s^2}q + \frac{\mathrm{d}^2q}{\mathrm{d}s^2}p\right) + \frac{\cos^2\theta + 2(1-\nu)n^2}{r^2}\frac{\mathrm{d}p}{\mathrm{d}s}\frac{\mathrm{d}q}{\mathrm{d}s} - \frac{n^2\cos\theta(3-2\nu)}{r^3}\left(\frac{\mathrm{d}q}{\mathrm{d}s}p + \frac{\mathrm{d}p}{\mathrm{d}s}q\right)\Bigg] + \left(\frac{1}{R_1^2} + \frac{\sin^2\theta}{r^2} + \frac{2\nu\sin\theta}{rR_1} + \frac{c^2n^4 + 2(1-\nu)c^2n^2\cos^2\theta}{r^4}\right) pq,$$

$\nu_1 \equiv (1-\nu)/2$, and θ is the angle between the outer normal to the midsurface and the symmetry axis Oz.

Furthermore, we use the Ritz method suggesting the following approximate solution:

$$u(s) = \sum_{j=1}^{N} x_j U_j(s), \quad v(s) = \sum_{j=1}^{N} x_{j+N} V_j(s), \quad w(s) = \sum_{j=1}^{N} x_{j+2N} W_j(s), \tag{17}$$

where x_j ($j = 1, 2, \ldots, 3N$) are unknown coefficients and $\{U_j\}$, $\{V_j\}$, and $\{W_j\}$ are sets of trial functions satisfying boundary conditions (4). Substituting (17) into (16) and setting $\delta u = U_k$, $\delta v = V_k$, and $\delta w = W_k$ yields the algebraic eigenvalue problem

$$(A - \lambda B)\mathbf{x} = \mathbf{0}, \quad \mathbf{x} \equiv (x_1, x_2, \ldots, x_{3N})^T, \tag{18}$$

with symmetric matrices A and B whose elements are

$$a_{i,j} = \int_{s_1}^{s_2} \Psi_{11}(U_j, U_i) r \mathrm{d}s, \qquad a_{i,j+N} = \int_{s_1}^{s_2} \Psi_{12}(V_j, U_i) r \mathrm{d}s, \qquad a_{i,j+2N} = \int_{s_1}^{s_2} \Psi_{13}(W_j, U_i) r \mathrm{d}s,$$

$$a_{i+N,j+N} = \int_{s_1}^{s_2} \Psi_{22}(V_j, V_i) r \mathrm{d}s, \qquad a_{i+N,j+2N} = \int_{s_1}^{s_2} \Psi_{23}(W_j, V_i) r \mathrm{d}s, \qquad a_{i+2N,j+2N} = \int_{s_1}^{s_2} \Psi_{33}(W_j, W_i) r \mathrm{d}s,$$

$$b_{i,j} = \int_{s_1}^{s_2} U_j U_i r \mathrm{d}s, \qquad b_{i+N,j+N} = \int_{s_1}^{s_2} V_j V_i r \mathrm{d}s, \qquad b_{i+2N,j+2N} = \int_{s_1}^{s_2} W_j W_i r \mathrm{d}s,$$

$$b_{i,j+N} = b_{i,j+2N} = b_{i+N,j+2N} = 0.$$

The trial functions should constitute a complete functional basis in an appropriate functional space with a mean-square metric involving their first- and second-order derivatives (Chap. 5 in [28]). This means that the Ritz method does not guarantee a uniform approximation of u, v, w, and their third- and fourth-order derivatives as N increases. Moreover, because the functional basis is not orthogonal, increasing N may lead to the ill-conditioned matrices A and B. As a consequence, whereas practical convergence demands a sufficiently large N, the Ritz method may become numerically unstable. To provide a fast and uniform convergence with a relatively small number of coordinate functions, the basis should possess the most important analytical properties of the eigenmodes.

Whereas the ratio h/R_0 decreases, parameter c^2 before K_{33} tends to zero and the governing ODEs become singularly perturbed. Therefore, the eigenmodes u, v, and w should exhibit the boundary layer behavior at the end of the interval $[s_1, s_2]$, that is, u, v, and w have both regular, slowly varying components and rapidly decaying components vanishing away from s_1 and s_2. Coordinate functions that capture the boundary layer behavior may provide the needed uniform convergence on $[s_1, s_2]$ (including higher-order derivatives) for intermediate and small values of c (see pp. 50–54 in [29]).

Henceforth, we employ the $(s - s_1)^{k_1}(s - s_2)^{k_2}$-weighted Legendre polynomials, satisfying the clamped-end conditions, and the boundary layer trial functions (14) and (15). For $w(s)$, the variational solution (17) is based on the functional set

$$\{W_i\}_{i=1}^{N} = \{W_1, \ldots, W_m; W_{m+1}, \ldots, W_{m+m_p}, \quad W_{m+m_p+1}, \ldots, W_{m+2m_p}; W_{m+2m_p+1}, \ldots, W_{m+3m_p}, W_{m+3m_p+1}, \ldots, W_{m+4m_p}\} \tag{19}$$

consisting of the five different families separated by the semicolons. The first family contains m functions represented by the weighted Legendre polynomials. The second and third families include m_p functions each, responsible for the boundary layer behavior at $s = s_1$, while the fourth and fifth families describe the same boundary layer behavior at $s = s_2$. Analogous functional sets are suggested for $u(s)$ and $v(s)$. Moreover, because $u(s)$ and $v(s)$ are restricted to the same boundary conditions, one can enforce $V_i = U_i$ $(i = 1, 2, \ldots, N)$.

The explicit expressions for $\{U_j\}$, $\{V_j\}$, and $\{W_j\}$ are as follows:

$$U_j(s) = (s - s_1)(s - s_2) P_j\left(\frac{2s}{l_s} - 1\right), \quad U_{m+1}(s) = g_{c_1} - 1 + \frac{s - s_1}{s_2 - s_1}, \quad U_{m+m_p+1}(s) = g_{s_1},$$

$$W_j(s) = (s - s_1)^2 (s - s_2)^2 P_j\left(\frac{2s}{l_s} - 1\right), \quad j = 1, 2, \ldots, m,$$

$$W_{m+1}(s) = g_{c_1} - 1 + \frac{s - s_1}{s_2 - s_1} - \frac{(s - s_1)(s - s_2)[p_1(s - s_1)(s_2 - s_1) + 1]}{(s_1 - s_2)(s_2 - s_1)} - \frac{(s - s_1)^2 (s - s_2)[p_1(s - s_1)(s_2 - s_1) + 2]}{(s_2 - s_1)^3},$$

$$W_{m+2}(s) = g_{c_1}(s - s_1) + \frac{(s - s_1)(s - s_2)}{(s_2 - s_1)} - \frac{(s - s_1)^2 (s - s_2)}{(s_2 - s_1)^2},$$

$$U_{m+j}(s) = g_{c_1}(s-s_1)s^{j-1}, \quad U_{m+m_p+j}(s) = g_{s_1}(s-s_1)s^{j-1},$$
$$U_{m+2m_p+1}(s) = g_{c_2} - \frac{s-s_1}{s_2-s_1}, \quad U_{m+2m_p+j}(s) = g_{c_2}(s-s_2)s^{j-1},$$
$$U_{m+3m_p+j}(s) = g_{s_2}(s-s_2)s^{j-1}, \quad U_{m+3m_p+1}(s) = g_{s_2}, \quad j = 2, 3, \ldots, m_p,$$
$$W_{m+m_p+1}(s) = g_{s_1} + \frac{p_1(s-s_1)^2(s-s_2)}{(s_2-s_1)} - \frac{p_1(s-s_1)^3(s-s_2)}{(s_2-s_1)^2},$$
$$W_{m+m_p+2}(s) = g_{s_1}(s-s_1), \quad W_{m+m_p+j}(s) = g_{s_1}(s-s_1)^2 s^{j-1},$$
$$W_{m+2m_p+1}(s) = g_{c_2} - \frac{(s-s_1)}{(s_2-s_1)} - \frac{(s-s_1)(s-s_2)}{(s_1-s_2)^2} - \frac{(s-s_1)^2(s-s_2)[p_2(s-s_2)(s_2-s_1)-2]}{(s_2-s_1)^3},$$
$$W_{m+2m_p+2}(s) = g_{c_2}(s-s_2) - \frac{(s-s_1)^2(s-s_2)}{(s_2-s_1)^2}, \quad W_{m+j}(s) = g_{c_1}(s-s_1)^2 s^{j-1},$$
$$W_{m+2m_p+j}(s) = g_{c_2}(s-s_2)^2 s^{j-1}, \quad W_{m+3m_p+1}(s) = g_{s_2} - \frac{p_2(s-s_1)^2(s-s_2)^2}{(s_2-s_1)^2},$$
$$W_{m+3m_p+2}(s) = g_{s_2}(s-s_2), \quad W_{m+3m_p+j}(s) = g_{s_2}(s-s_2)^2 s^{j-1}, \ j = 3, 4, \ldots, m_p,$$

where

$$l_s \equiv s_2 - s_1; \quad b_{0,k}(\lambda) \equiv \lambda - \frac{1-\nu^2}{R_2^2(s_k)}, \quad p_k \equiv p_k(\lambda) = \frac{(-1)^k |b_{0,k}(\lambda)|^{1/4}}{\mu\sqrt{2}}$$
$$g_{c_k} \equiv e^{p_k(s-s_k)} \cos p_k(s-s_k), \quad g_{s_k} \equiv e^{p_k(s-s_k)} \sin p_k(s-s_k), \quad k = 1, 2. \tag{20}$$

In the preceding equations, the functions $P_j(s)$ denote the Legendre polynomials, which can be computed directly or by adopting the Bonnet recursive formulas.

Whereas $m_p > 0$, parameters p_k in (20) are functions of λ, and therefore problem (18) is nonlinearly dependent on λ. To solve (18), one can use the fact that the purely regular basis, that is, the case $m_p = 0$, gives a quite good approximation of λ (but not the eigenmodes!). This means that an iterative algorithm may start with $m_p = 0$ (without the correcting boundary layer-type functions) and a purely linear statement of (18) to find an initial approximation of λ. By substituting this value into the formulas for $m_p > 0$, one can find a new approximation of λ and the corresponding eigenmodes by solving the matrix spectral problem (18). The newly found λ is used for the next iteration, and so on.

4 Convergence analysis, numerical experiments, and validation

Our focus is on cylindrical and conical shells admitting the parameterization

$$s = \frac{l-z}{\cos\alpha}, \quad r(s) = 1 + s\sin\alpha, \quad \theta = \frac{\pi}{2} - \alpha, \quad \frac{1}{R_1} = 0, \tag{21}$$

where l and α are the nondimensional shell height (projection of shell length on the Oz-axis) and the semiapex angle ($\alpha = 0$ for a cylindrical shell), respectively. For cylindrical shells, l implies the nondimensional shell length. The ratio of the shell radius R_{s_1} at $s = s_1$ to the shell thickness is denoted by $\delta = R_{s_1}/h$. Numerical results are reported for $n = 1$ (first antisymmetric modes, "beam type" modes, bending modes).

Tables 1 and 2 are devoted to the cylindrical shell case. Table 1 demonstrates a typical convergence to the three-nondimensional natural frequencies $\omega_i = \sqrt{\lambda_i}$, $i = 1, 2, 3$, of the bending modes as well as the normal deflections and their derivatives. The derivatives are computed at a point whose distance to the shell end is 1% of the shell length ($z^* = z/l = 0.99$ in calculations). We fix $m_p = 2$ but increase the number of the Legendre polynomials, m, from 2 to 14. The table shows a rapid stabilization of the ten significant figures for the eigenfrequencies. At least four significant figures are also stabilized for the normal deflections w_i and their derivatives. The convergence

Table 1 Convergence to nondimensional eigenfrequencies (ω_i), eigenmodes, and their derivatives computed in a neighborhood of the shell edge

m	ω_i	w_i	w_i'	w_i''	w_i'''	w_i''''
$i = 1$						
2	0.308517870	0.078491224	1.94629204	−49.2411	−487.1545	214,694.6
4	0.305471542	0.073404538	1.82463596	−41.1166	−372.7503	157,571.2
6	0.305466854	0.073336305	1.82233157	−41.3056	−373.4445	159,370.3
8	0.305466852	0.073334715	1.82230788	−41.3002	−373.4579	159,328.0
10	0.305466852	0.073334712	1.82230756	−41.3002	−373.4571	159,328.4
12	0.305466852	0.073334712	1.82230756	−41.3002	−373.4571	159,328.4
$i = 2$						
2	0.586145017	−0.06180331	−2.3513934	39.979	4,031.075	−409,828
4	0.573173561	−0.05370921	−1.8803672	−8.3382	658.7091	−22,648
6	0.573034958	−0.05432720	−1.9245913	−1.3104	1,112.712	−77,168
8	0.573034593	−0.05429076	−1.9222202	−1.7433	1,087.452	−73,778
10	0.573034592	−0.05429182	−1.9222798	−1.7287	1,088.174	−73,893
12	0.573034592	−0.05429179	−1.9222787	−1.7290	1,088.161	−73,890
14	0.573034592	−0.05429179	−1.9222787	−1.7290	1,088.161	-73,890
$i = 3$						
2	0.883718637	-7×10^{-9}	2×10^{12}	-1×10^{13}	-2×10^{15}	7×10^{16}
4	0.774417089	−0.104089	4.07655	1.1506	4,020.9	286,538
6	0.759725088	−0.073384	2.76494	17.021	1,460.9	48,932
8	0.759391036	−0.071862	2.71864	12.825	1,657.9	78,466
10	0.759388888	−0.071696	2.71191	13.158	1,637.3	75,412
12	0.759388882	−0.071694	2.71184	13.137	1,638.0	75,572
14	0.759388882	−0.071694	2.71184	13.137	1,638.0	75,565

The first three bending modes ($n = 1, i = 1, 2, 3$) for a cylindrical shell with $\delta = 1{,}000$ and the Poisson coefficient $\nu = 0.3$. The eigenmodes and their first to fourth derivatives, $w_i, w_i', \ldots, w_i''''$, are presented at the point $z^* = 0.99(z^* = z/l)$, where l is the shell height (length) as defined in (21). The number of Legendre polynomials m in (19) increases, but the number of boundary layer trial functions is always fixed, $m_p = 2$

is slower for the third- and fourth-order derivatives. Table 2 shows analogous results for the first eigenmode with $\delta = 100$ and $\delta = 2{,}000$, confirming the fact that the accuracy is not affected by the shell thickness.

To demonstrate that the method provides a uniform convergence to the eigenmodes on the entire interval $0 < z^* < 1$, we introduce the error functions $\varepsilon_i = \varepsilon_i(z^*)$, $i = 1, 2, 3$ (the eigenmodes are scaled to reach a maximum displacement equal to 1) that characterize the errors in satisfying the three governing ODEs (2). Figure 2 shows the typical behavior of $\varepsilon_i = \varepsilon_i(z^*)$, $i = 1, 2, 3$, for $m = 16$ and $m_p = 0$ (purely regular basis) versus the case with $m = 16$ and $m_p = 2$ (two boundary layer functions are used). The figure shows that using Legendre polynomials with $m_p = 0$ gives a maximum uniform error equal to 0.1, but incorporating the two boundary layer-type functions improves the convergence so that the maximum uniform error equals 4×10^{-9}.

Our semianalytical approach can be validated using the asymptotic results in [17] and finite-element computations. Nau and Simmons [17] constructed an asymptotic approximation of the eigensolution for the Koiter cylindrical shell with clamped edges. As we remarked in Sect. 1, this is not the same as the technical theory of shells. However, Table 5, which presents a comparison of the eigenvalues following from our semianalytical approximation and

Table 2 The same as in Table 1, but for $\delta = 100$ and $\delta = 2{,}000$

m	ω_1	w_1	w_1'	w_1''	w_1'''	w_1''''
$\delta = 100$						
2	0.307311264	0.02252671	0.995807	15.2577	−450.78	3,971.5
4	0.305888225	0.02220086	0.957923	13.4822	−430.34	6,712.7
6	0.305886926	0.02217318	0.957495	13.5140	−430.49	6,613.6
8	0.305886926	0.02217323	0.957486	13.5134	−430.47	6,614.9
10	0.305886926	0.02217323	0.957486	13.5134	−430.47	6,614.9
12	0.305886926	0.02217323	0.957486	13.5134	−430.47	6,614.9
$\delta = 2{,}000$						
2	0.308791219	0.09326250	1.3600325	−72.722637	3,868.800	118,159.9
4	0.305439921	0.08763065	1.3531353	−64.163059	2,832.105	81,459.66
6	0.305434417	0.08750605	1.3477016	−64.215450	2,866.972	82,253.77
8	0.305434415	0.08750464	1.3477495	−64.212269	2,866.097	82,241.17
10	0.305434415	0.08750463	1.3477485	−64.212274	2,866.106	82,241.19
12	0.305434415	0.08750463	1.3477485	−64.212274	2,866.106	82,241.19

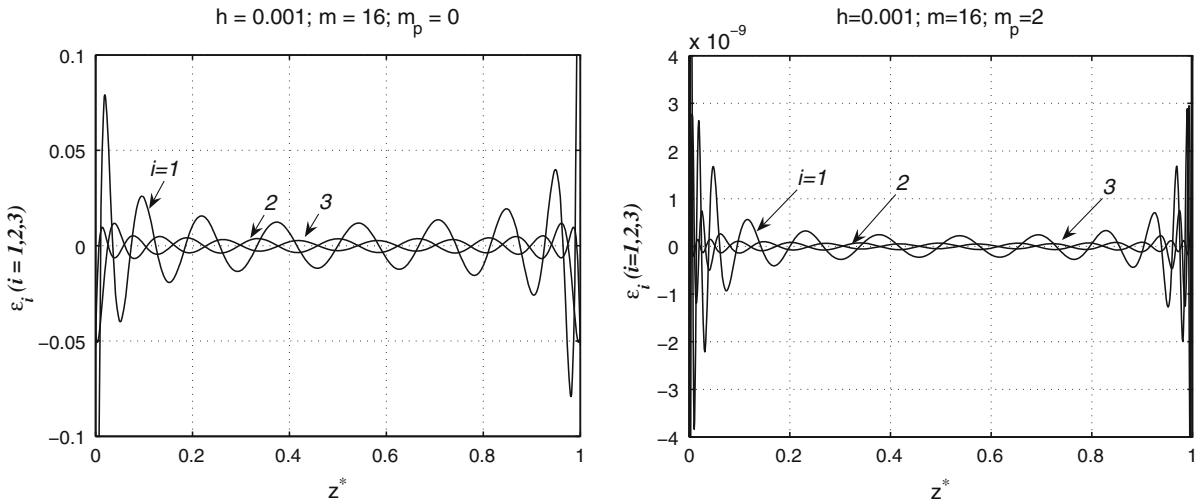

Fig. 2 Error functions $\varepsilon_i(z^*)$ for cylindrical shell with $\delta = 1{,}000$ and $\nu = 0.3$; the first bending eigenmodes

numerical results from [17], shows that the eigenfrequencies by different theories and methods are close to each other. Our computations were made with $m = 16$ and $m_p = 2$. The nondimensional frequencies ω_i are linked to the normalized values Λ_i in [17] by the formula $\Lambda_i = \omega_i^2/(1-\nu^2)$.

The method demonstrates a slightly slower convergence for conical shells. Table 3 illustrates this fact for the three lower eigenfrequencies (bending eigenmodes, $n = 1$) and the two different shell heights, $l = 20$ and $l = 30$, respectively, with $\delta = 2{,}000$ and $\alpha = 15°$. The four to five significant figures are stabilized for eigenfrequencies with $m_p = 2$ and $m = 16$. The convergence becomes slower with increasing l. Table 3 shows that when $l = 20$, we need $m = 10$ to stabilize the six significant figures, whereas the case $l = 30$ requires $m = 18$ to stabilize the four significant figures.

Table 3 Convergence to the three lowest nondimensional frequencies for the beam-type eigenmodes ($n = 1$)

m	$l = 20$			$l = 30$		
	ω_1	ω_2	ω_3	ω_1	ω_2	ω_3
2	0.059030	0.111711	0.146790	0.038377	0.074419	0.103706
4	0.057773	0.105058	0.144611	0.037463	0.068582	0.099733
6	0.057679	0.104800	0.143988	0.037363	0.068313	0.098588
8	0.057672	0.104789	0.143981	0.037351	0.068287	0.098567
10	0.057671	0.104788	0.143978	0.037348	0.068282	0.098562
12	0.057671	0.104788	0.143978	0.037345	0.068279	0.098559
14	0.057671	0.104788	0.143978	0.037340	0.068274	0.098557
16	0.057671	0.104788	0.143978	0.037335	0.068269	0.098554

Conical shell with $R_{s_1}/h = \delta = 2{,}000$ and two different nondimensional shell heights, $l = 20$ and $l = 30$, respectively. The semiapex angle is $\alpha = 15°$; Poisson coefficient equals 0.3. Integer m implies the number of Legendre polynomials in (19); $m_p = 2$

Table 4 Convergence to lowest eigenfrequency $\omega_{\min} = \min\limits_{n,i} \omega_{ni} = \min\limits_{n,i} \sqrt{\lambda_{ni}}$

	$\omega_{\min}$			
	$\delta = 100, n = 7$	$\delta = 400, n = 11$	$\delta = 1{,}000, n = 12$	$\delta = 2{,}000, n = 15$
2	0.0494923	0.0285036	0.0183033	0.0137052
4	0.0481154	0.0260378	0.0161554	0.0115560
6	0.0481085	0.0259863	0.0161529	0.0115525
8	0.0481084	0.0259860	0.0161528	0.0115523
10	0.0481084	0.0259860	0.0161527	0.0115523
12	0.0481084	0.0259860	0.0161527	0.0115523

Conical shell with different values of $R_{s_1}/h = \delta$. Furthermore, $l = 4$, the semiapex angle $\alpha = 30°$, and the Poisson coefficient is $\nu = 0.3$. Integer m implies the number of Legendre polynomials, but $m_p = 2$

Our numerical studies show that increasing the semiapex angle α does not affect the convergence. For conical shells with $l = 4$, $\alpha = 30°$, and different thicknesses, Table 4 shows the convergence to the lowest eigenfrequency $\omega_{\min} = \min\limits_{n,i} \omega_{ni} = \min\limits_{n,i} \sqrt{\lambda_{ni}}$. As long as l is sufficiently small, the method provides a fast convergence to this eigenfrequency, and this result is not affected by the shell thickness. Figure 3 demonstrates the behavior of $w_1(z^*)$ and its derivatives in a neighborhood of the clamped end for $\alpha = 30°$. When the shell thickness decreases, a clear slope zone is observed.

We have tried to validate our method by comparison with finite-element calculations. ANSYS codes were used that utilize a fully three-dimensional finite-element scheme. The codes return the lowest dimensional eigenfrequencies, but the shared-codes version does not provide an information on the eigenmodes (on the integer numbers n and i). The lowest 6 (12, since two antisymmetric modes correspond to each eigenfrequency) eigenfrequencies are presented in Table 6. These eigenfrequencies correspond to different n, not only $n = 1$ as in the previous numerical examples. The table illustrates that there is a discrepancy between our approximation and the ANSYS results with increasing shell thickness. However, the discrepancy for lower thicknesses is relatively small, less than 1%. Unfortunately, the shared version of the ANSYS codes does not provide an output on deflections and associated bending force and moment.

Table 5 Comparison of eigenfrequencies for cylindrical shell following from our approximation within the framework of the technical theory of shells and those in [17] computed by an asymptotic method for the Koiter shell equations

i	$n=1$		$n=2$		$n=3$	
	Λ_i	$\omega_i^2/(1-\nu^2)$	Λ_i	$\omega_i^2/(1-\nu^2)$	Λ_i	$\omega_i^2/(1-\nu^2)$
1	0.06297	0.062985499	0.01746	0.017472752	0.00570	0.005706639
2	0.23623	0.236229128	0.07909	0.079102303	0.03043	0.030441250
3	0.48434	0.484341709	0.19350	0.193516205	0.08365	0.083669845
4	0.67091	0.670936785	0.33380	0.333809915	0.16324	0.163262364
5	0.71864	0.719243011	0.46780	0.467804162	0.25856	0.258572274
6	0.78434	0.784341168	0.57851	0.578507924	0.35650	0.356511174
i	$n=4$		$n=5$			
	Λ_i	$\omega_i^2/(1-\nu^2)$	Λ_i	$\omega_i^2/(1-\nu^2)$		
1	0.00225	0.002248236	0.00103	0.001030554		
2	0.001338	0.013385540	0.00657	0.006578651		
3	0.04002	0.040033110	0.02090	0.020914759		
4	0.08451	0.084531225	0.04669	0.046712749		
5	0.14487	0.144894267	0.08452	0.084548435		
6	0.21575	0.215772921	0.13287	0.132899664		

The nondimensional shell thickness is 0.0001, and the nondimensional shell length is 5 (normalization by shell radius R_{s_1}). The value Λ_i in [17] is the same as $\omega_i^2/(1-\nu^2)$ in our consideration

Table 6 Six lowest eigenfrequencies of cylindrical shell, $\sqrt{\lambda_i}$, $i=1,\ldots,6$, obtained by means of present semianalytical method, and lowest eigenfrequencies $\sqrt{\lambda_i^*}$ computed using ANSYS codes based on finite-element method

m	$\sqrt{\lambda}$ (Hz) $h=0.01$ (m)	$\sqrt{\lambda^*}$ (Hz)	n	i	m	$\sqrt{\lambda}$ (Hz) $h=0.001$ (m)	$\sqrt{\lambda^*}$ (Hz)	n	i
1	69.731	68.354	4	1	1	23.059	22.889	8	1
2	73.655	71.579	5	1	2	24.117	23.905	9	1
3	91.041	90.467	3	1	3	24.667	24.550	7	1
4	93.842	91.478	6	1	4	27.057	26.816	10	1
5	117.367	115.950	5	2	5	29.789	29.722	6	1
6	123.359	116.584	7	1	6	31.279	31.019	11	1
m	$\sqrt{\lambda}$ (Hz) $h=0.0005$ (m)	$\sqrt{\lambda^*}$ (Hz)	n	i					
1	16.522	16.428	10	1					
2	16.731	16.661	9	1					
3	17.519	17.406	11	1					
4	18.516	18.471	8	1					
5	19.393	19.256	12	1					
6	21.898	21.757	13	1					

The dimensional eigenvalues are presented for dimensional shell thickness h as $l=4$ (m), $R_0=R_{s_1}=1$ (m), $E=2\times10^{11}$ (Pa), and $\rho=8\times10^3(\mathrm{kg/m^3})$

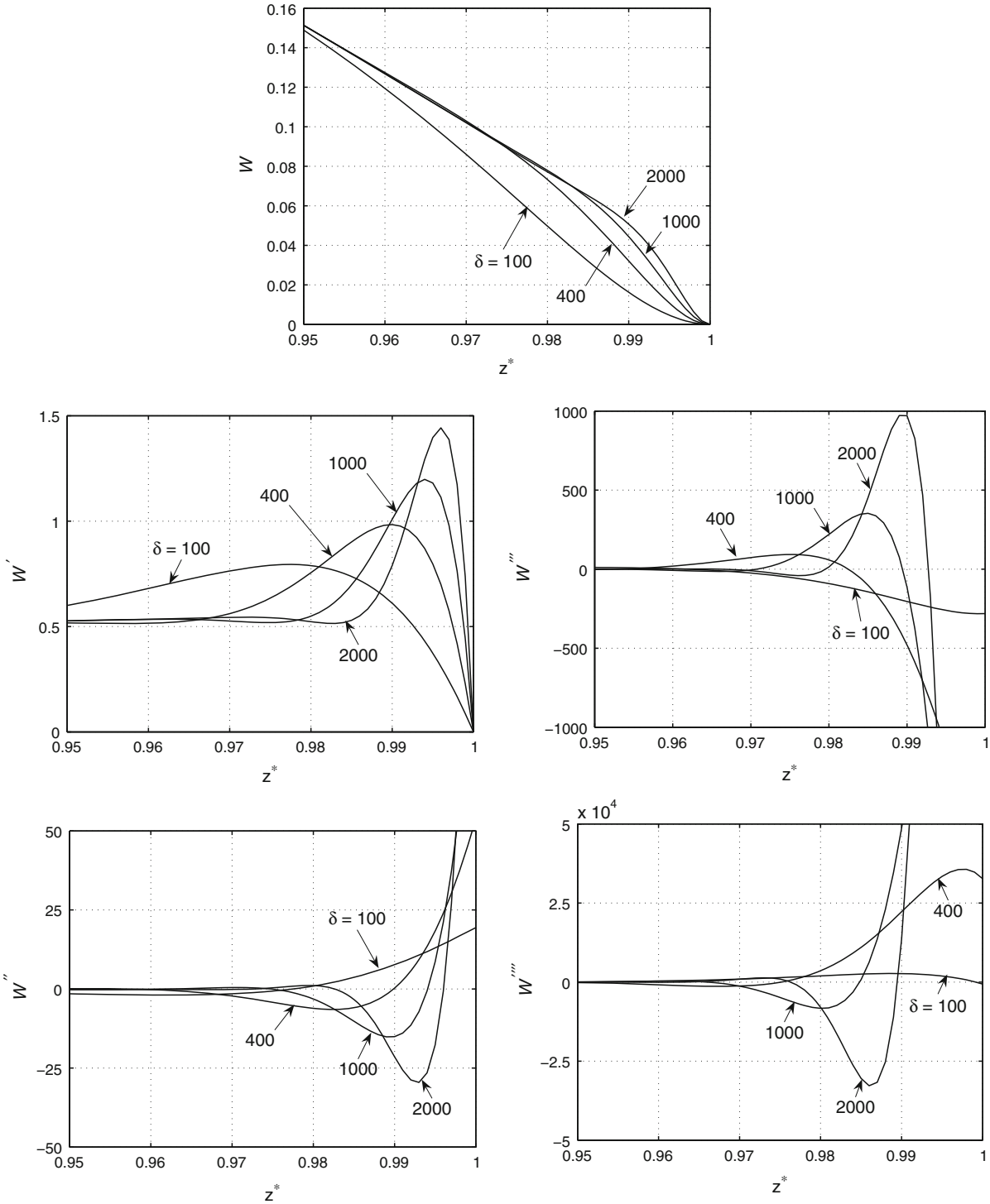

Fig. 3 Behavior of $w_1(z^*)$ and its four derivatives in neighborhood of clamped shell end for conical shell with $\alpha = 30°$

5 Concluding remarks

In [1], we proposed a semianalytical approach to describe axisymmetric oscillations of a thin-walled cupola-shaped shell. The analysis included a study of the eigenmode behavior, constructed of special set of trial functions possessing this behavior, and developed the corresponding Ritz scheme. These analytical and numerical results are generalized in the present paper for the case of azimuthally closed, radially open shells. As in [1], the technical theory of shells and the clamped end conditions are adopted. The developed Ritz scheme provides a fast convergence to both eigenfrequencies and modes. The convergence to the eigenmodes is in a uniform metric so that both deflections and their up-to-fourth derivatives are accurately approximated on the entire interval $[s_1, s_2]$. This should provide a good approximation of bending forces and moment in the vicinity of the shell edges. The convergence was illustrated in numerical experiments where the focus was on cylindrical and conical shells. The method accuracy is, generally, not affected by shell thickness. For conical shells, the convergence may become slower for longer shells, but the semiapex angle does not influence the accuracy.

Our analytically approximate results were validated by comparison with finite-element calculations using ANSYS codes. The latter codes are based on the fully three-dimensional statement; thus, as was expected, the approximate eigenfrequencies by these two methods become close with decreasing shell thickness. In the asymptotic limit by the nondimensional shell thickness, we used the Nau and Simmonds [17] solution to validate our results. Even though [17] employed the Koiter equation of shells, our analysis was based on the technical theory of shells, and the eigenfrequencies for the bending modes obtained by the two methods remain very close, especially with decreasing shell thickness.

Acknowledgment The authors thank the German Research Society (DFG) for its financial support.

References

1. Gavrilyuk I, Hermann M, Trotsenko V, Trotsenko Yu, Timokha A (2010) Axisymmetric oscillations of a cupola-shaped shell. J Eng Math 65:165–178
2. Leissa AW (1993) Vibration of shells. Acoustical Society of America, New York
3. Anderson GL (1970) On Gegenbauer transforms and forced torsional vibrations of thin spherical shells. J Sound Vib 12:265–275
4. Göller B (1980) Dynamic deformations of thin spherical shells based on analytical solutions. J Sound Vib 73:585–596
5. Mukherjee K, Chakraborty SK (1985) Exact solution for larger amplitude free and forced oscillation of a thin spherical shell. J Sound Vib 100:339–342
6. Al-Jumaily AM, Najim FM (1997) An approximation to the vibrations of oblate spheroidal shells. J Sound Vib 207:561–574
7. Reissner E (1941) A new derivation of the equations for the deformation of elastic shells. Am J Math 62(1):177–184
8. Mushtari KhM, Galimov KZ (1957) Non-linear theory of thin elastic shells. NASA Technical Report, NASA-TT-F-62, Washington, DC
9. Mushtari KhM, Sachenkov AV (1958) Stability of cylindrical and conical shells of circular cross section, with simultaneous action of axial compression and external normal pressure. NACA Technical Memorandum, NACA TM 1433, Washington, DC
10. Reissner E, Wan FYM (1969) On the equations of linear shallow shell theory. Stud Appl Math 48:133–145
11. Koiter WT (1966) Summary of equations for modified, simplest possible accurate linear theory of thin circular cylindrical shells. Rep 442, Lab Tech Mech, TH, Delft
12. Koiter WT (1966) On the nonlinear theory of thin elastic shells. I-Introductory sections. II: Basic shell equations. III: Simplified shell equations. Koninklijke Nederlandse Akademie van Wetenschappen, Proceedings, Series B 69(1):1–54
13. Green AE, Naghdi PM (1968) The linear elastic cosserat surface and shell theory. Int J Solids Struct 4:585–592
14. Ilgamov MA (1969) Oscillations of elastic shells containing liquid and gas. Nauka, Moscow (in Russian)
15. Libai A, Simmonds JG (1998) Nonlinear theory of elastic shells. Cambridge University Press, Cambridge, UK
16. Ross EW Jr (1966) Asymptotic analysis of the axisymmetric vibration of shells. J Appl Mech 33:553–561
17. Nau RW, Simmonds JG (1973) Calculation of the low natural frequencies of clamped cylindrical shells by asymptotic methods. Int J Solids Struct 9:591–605
18. Vlasov VZ (1949) General theory of shells and its application in technology. Gostechizdat, Moscow (in Russian)
19. Gavrilyuk I, Hermann M, Trotsenko Yu, Timokha A (2010) Eigenoscillations of three- and two-element flexible systems. Int J Solids Struct 47:1857–1870
20. Wasow W (2002) Asymptotic expansions for ordinary differential equations. Dover, New York

21. Verhulst F (2005) Methods and applications of singular perturbations: boundary layers and multiple timescale dynamics. Springer Science+Business Media, New York
22. O'Malley RE Jr (1991) Singular perturbation methods for ordinary differential equations. Springer Science, New York
23. Goldenveizer AL, Lidski VB, Tovstik PE (1979) Free vibrations of thin elastic shells. Nauka, Moscow (in Russian)
24. Alumyan NA (1960) On fundamental system of integrals of equation on small axisymmetric steady-state oscillations of an elastic conical shell of revolution. Izv AN Est SSR, Ser Technol Phys Math Sci 10(1):3–15 (in Russian)
25. Lubimov VM, Pshenichnov GI (1976) The perturbation method in shallow shell theory. Mech Solids 11(4):120–124
26. Tovstik PE (1975) Low-frequency oscillations of a convex shell of revolution. Izv AN SSSR, Mech Solid Bodies 6:110–116 (in Russian)
27. Vishik MI, Lusternik LA (1957) Regular degeneracy and boundary layer for linear differential equations with a small parameter. Uspekhi Math Nauk 12(5):3–122
28. Marchuk GI (1982) Methods of numerical mathematics, 2nd edn. Springer, New York
29. Doolan EP, Miller JJH, Schilders WHA (1980) Uniform numerical methods for problems with initial and boundary layers. Boole Press, Dublin